A Comparative Study of *In-Situ* Composite Fibers Reinforced with Different Rigid Liquid Crystalline Polymers

LIHUA PAN, BORUN LIANG

Department of Polymeric Materials Engineering, China Textile University, Shanghai 200051 People's Republic of China

Received 3 June 1997; accepted 18 April 1998

ABSTRACT: Poly(ethylene terephthalate) (PET) and 2 thermotropic liquid crystalline polymers (LCPs) with different chain rigidity were blended to make *in-situ* composite fibers on a conventional melt spinning equipment. The addition of the LCP-1 (60PHB–PET) with a less rigid chain has been found to lower the orientation of the as-spun fibers while the LCP-2 (VectraA900) with whole aromatic rigid chain has a reverse effect, as evidenced from the birefringence results. Both kinds of composite fibers with 5 wt % LCP have a good drawability. There is a diffraction peak characteristic of intermolecular packing of LCP on the wide-angle X-ray diffraction curve for the as-spun fibers containing LCP-2 but not the case for LCP-1. The morphology formed during elongational flow is highly dependent on the composition and rigidity of LCP. For the dispersed phases of LCP-1, it is relatively difficult to be elongated, whereas LCP-2 dispersed phases will be easily deformed into fibrils during melt spinning. The mechanical properties of the blend fibers containing the LCP-1 component are inferior to those containing the LCP-2 component. For the fibers with discontinuous fibril morphology, a Halpin–Tsai equation could well be used to describe the elastic modulus of *in-situ* composite fiber with LCP-2. © 1998 John Wiley & Sons, Inc. J Appl Polym Sci 70: 1035–1045, 1998

INTRODUCTION

In recent years, conventional thermoplastic polymers (TPs) have been blended with thermotropic liquid crystalline (LC) copolymers in an attempt to improve the strength and modulus of matrix TPs. An obvious advantage of LC polymers (LCP) as an additive over an isotropic one is that most LCPs have an intrinsically low melt viscosities in the nematic phase and a strong tendency of easy orientation along the flow direction. LCPs usually consist of rigid rod-like molecular chains and exist as ordered domains in the LC state. These ordered domains in the blend melt could be preferentially oriented during elongational flow in the melt processing, which could act as a reinforcing agent similar to glass fiber; they are called *in-situ* composites.[1] The mechanical properties of blends, therefore, are directly affected by the supermolecular structure and morphology of the blends, mainly including the shape of dispersed phases and the orientation of LCP and the interfacial adhesion between the 2 phases.

Many articles have involved the blends of LCPs with poly(ethylene terephthalate).[2–6] In some cases, the strength and moduli of the PET blends

Correspondence to: L. Pan.

Journal of Applied Polymer Science, Vol. 70, 1035–1045 (1998)
 CCC 0021-8995/98/051035-11

Table I Composition of the PET–LCP *In-Situ* Composite Fibers

Sample Code	PET-1 (wt %)	PET-2 (wt %)	LCP-1 (wt %)	LCP-2 (wt %)
95PET-1–5LCP-1	95		5	
90PET-1–10LCP-1	90		10	
80PET-1–20LCP-1	80		20	
95PET-1–5LCP-2	95			5
90PET-1–10LCP-2	90			10
80PET-1–20LCP-2	80			20
95PET-2–5LCP-2		95		5
90PET-2–10LCP-2		90		10
80PET-2–20LCP-2		80		20
50PET-2–50LCP-2		50		50
20PET-2–80LCP-2		20		80
10PET-2–90LCP-2		10		90

are found to follow a linear mixture rule, resulting in substantial increases in strength and stiffness.[4] But the extent of improvement is highly dependent on the processing history of the blends.[7] In our previous study,[8] the PET as-spun blend fibers with VectraA900 had a significant increase in modulus but just a slight increase in strength. Blend fibers with 10 wt % 60PHB–PET and 90 wt % PET exhibited significant increase in modulus from 1.9 to 2.5 GPa and tensile strength from 60.5 to 67.8 MPa.[2]

The objective of this study is mainly to investigate the effect of the LCPs with different rigid chain on the orientation, crystalline structure, and morphology of PET–LCP *in-situ* composite fibers and, hence, their mechanical properties. In addition, the moduli measured of PET–LCP-2 composite fibers are compared with the calculated values based on the Halpin–Tsai model in order to ensure the degree of fibril formation.

EXPERIMENTAL

Materials

The PET used in the composite fibers was provided by China Yizheng Chemical Fiber Co. with an intrinsic viscosity of 0.64 dL/g designated as PET-1, and by Japan Toyobo Co. with the intrinsic viscosity of 1.0 dL/g as PET-2, respectively. LCP pellets used were 60PHB–PET (LCP-1), supplied by China Chengdu Organic Silicon Research Center and VectraA900 (LCP-2) produced by Hoechst Celanese Co.

Spinning and Drawing

Dry blending was performed for the predetermined compositions shown in Table I. Melt spinning was carried out on a FUJI FILTER MSTC-400 melt spinning machine made in Japan with a 28-hole ($d = 0.5$ mm) spinneret. The pump output was 15 g/min. Blend fibers were made at 290–300°C and at a take-up speed of $\sim$ 400 m/min, with the corresponding draw down ratio of $\sim$ 215. The as-spun filaments were drawn by two-stage drawing.

Characterization

The orientation factor of sonic velocity f_s was measured on a SOD-II sonic velocity measuring

Table II The Composition Effect on the Orientation of PET-1–LCP-1 As-Spun Fibers

PET-1–LCP-1	C (km/s)	f_s (%)	Δn ($\times 10^{-3}$)
100/0	1.42	9.6	13.35
95/5	1.27	11.0	10.61
90/10	1.35	39.2	8.24
80/20	1.44	72.0	7.41

Table III The Relationship Between the Drawdown Ratio and the Orientation of 95PET-1–5LCP-1 As-Spun Fiber

V_L/V_0	C (km/s)	f_s (%)	Δn ($\times 10^{-3}$)
68	1.27	11.0	8.19
102	1.27	11.0	10.61
136	1.30	14.3	12.48
170	1.32	17.0	13.62

Table IV The Orientation of PET-2–LCP-2 As-Spun Fibers

PET-2–LCP-2	V_L/V_0	f_s (%)	Δn ($\times 10^{-3}$)
100/0	107	5.7	3.62
	161	2.9	3.57
95/5	107	22.0	6.65
	161	31.4	8.04
	215	—	9.36
90/10	107	65.4	5.02
	161	65.7	7.16
80/20	107	73.9	6.77
50/50	107	95.0	—
0/100	68	98.0	10.51

Table V The Orientation of Drawn Blend Fibers

Sample	V_L/V_0	Draw Ratio	f_s (%)
95PET-1–5LCP-1	68	0	11.0
		2.7	63.0
		3.0	64.1
		3.2	72.1
		3.4	74.9
	102	0	11.0
		2.0	34.8
		2.7	63.5
		3.0	66.7
		3.2	74.1
		3.4	78.3
95PET-2–5LCP-2	107	3.0	76.0
	161	3.0	75.2
	215	3.0	79.4

instrument for blend fibers. The f_s value of the fiber was calculated as follows:

$$f_s = 1 - Cu^2/C^2$$

where Cu and C are the sonic velocity of unoriented and oriented samples, respectively.

Birefringence Δn of the blend fibers was measured on a polarizing microscope with a compensator, and the Δn values were averaged with 7 times measurements for each sample.

Wide-angle X-ray diffraction patterns (WAXD) were measured with cut fiber powder on a D/max RB-II X-ray diffractometer.

The phase morphology of the blend fibers was observed on a CamScan-4 high-resolution scanning electron microscope. The sample measured were broken in the liquid nitrogen and then the fracture surfaces were sputter-coated in vacuum with a gold–palladium alloy to prevent charging in the electron beam.

The mechanical properties were examined on a YG-00A electric tensile tester. The values were averaged for 10 test samples.

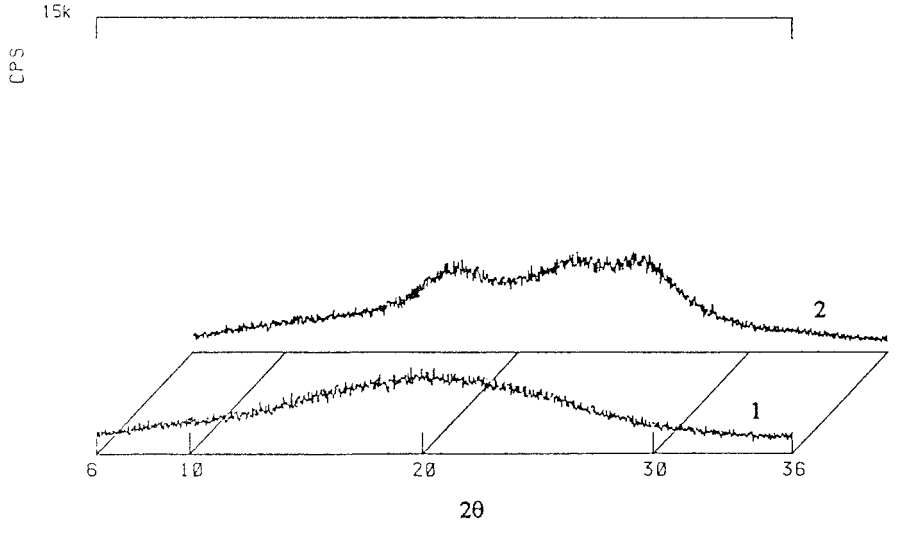

Figure 1 WAXD curves for 95PET-1–5LCP-1 fibers before and after drawing: (1) as-spun fiber (V_L/V_0 = 102); (2) drawn fiber (R = 3.0).

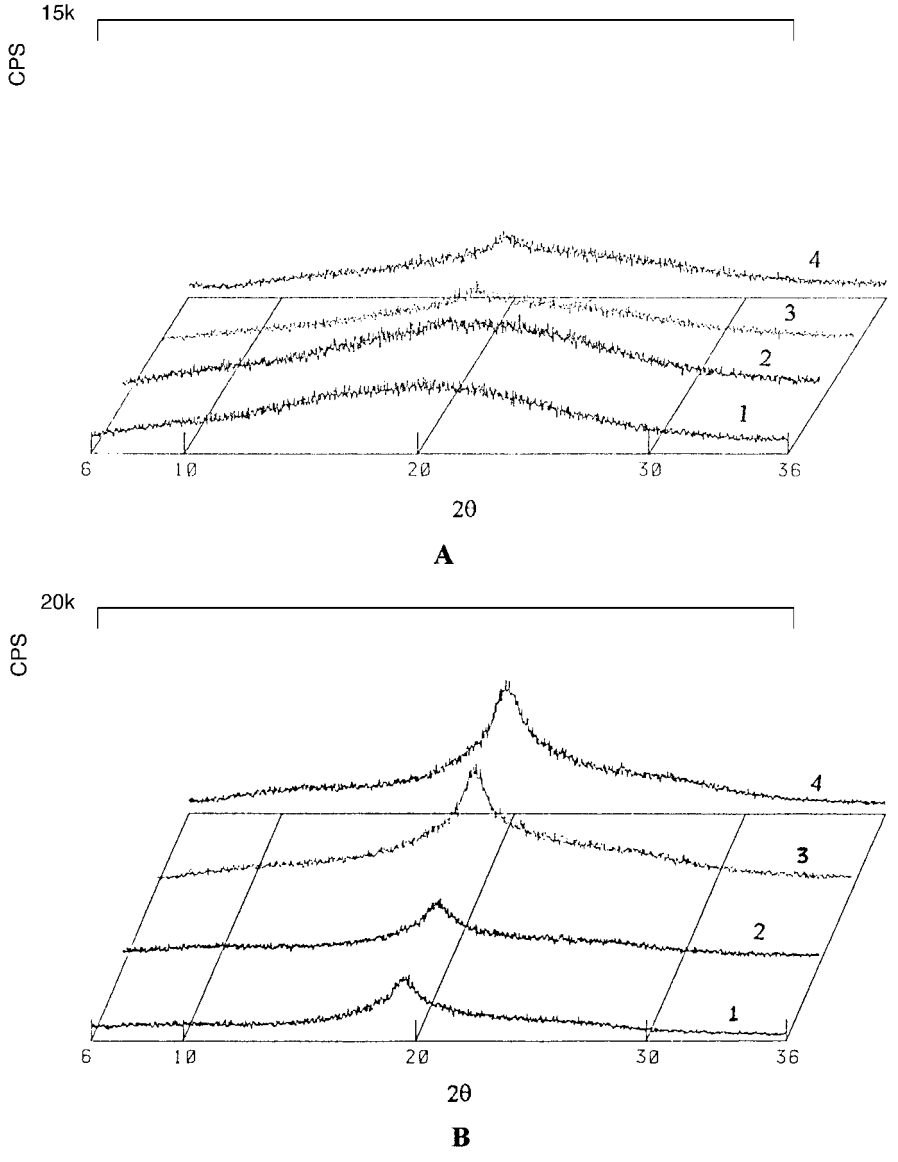

Figure 2 WAXD curves for PET-2–LCP-2 as-spun fibers: (A) (1) 100/0; (2) 95/5; (3) 90/10; (4) 80/20. (B) (1) 50/50; (2) 20/80; (3) 10/90; (4) 0/100.

RESULTS AND DISCUSSION

Orientation of Fibers

The composition effect on the orientation of PET-1–LCP-1 blend fibers, measured as f_s and birefringence, respectively, is shown in Table II. From the results of sonic velocity measurements, it can be seen that the as-spun blend fibers with increasing LCP amount have higher f_s values, owing to the higher sonic modulus of LCP rod-like molecular chain. However, birefringence measurement shows an opposite tendency; that is, LCP-1 considerably lowers the orientation of as-spun blend fibers, and, therefore, PET-1–LCP-1 blend fibers have a substantially low birefringence value compared to the control PET fiber. This phenomenon was also observed by Brody[9] at high wind-up speed (WUS). Adding a small amount of LCP in the blend will result in that fibers spun at high WUS appear as if they were

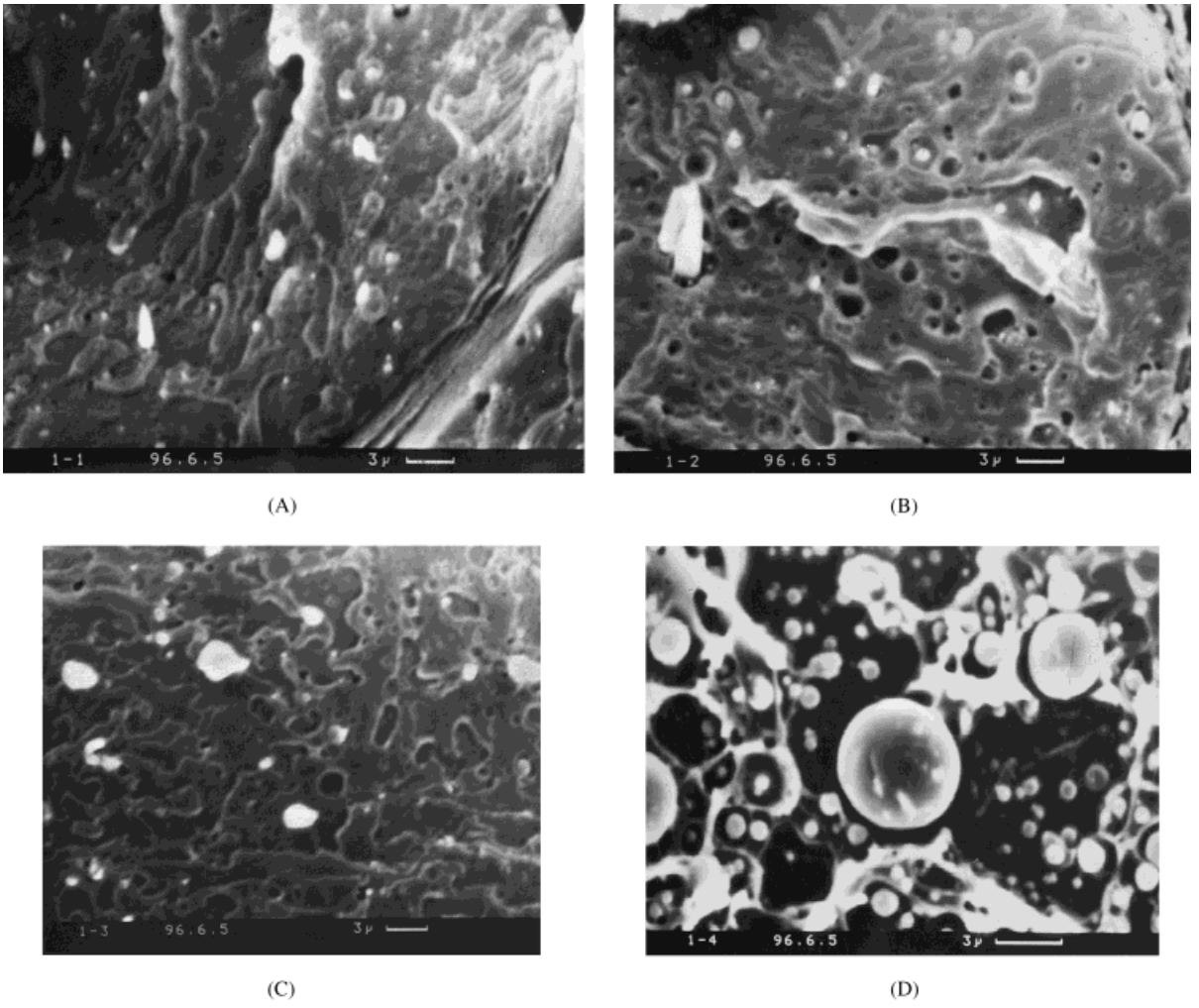

Figure 3 SEM photographs for PET-1–LCP-1 as-spun fibers at the cross section. (A) 95PET-1–5LCP-1 (V_L/V_0 = 68). (B) 95PET-1–5LCP-1 (V_L/V_0 = 136). (C) 90PET-1–10LCP-1 (V_L/V_0 = 68). (D) 80PET-1–20LCP-1 (V_L/V_0 = 25).

spun at a lower WUS, and the effect has been termed WUS suppression (WUSS). In our cases, although the wind-up speed was not high, the morphological change of blend fibers in the elongational flow along the spinning line was similar to that of fibers studied by Brody.

Table III shows the effect of drawdown ratio on the orientation of blend fiber at the composition of 95PET-1–5LCP-1. With increasing drawdown ratio, both the f_s and Δn values of the fiber monotonically increase. It is considered that the ordered domains of LCP could preferentially form oriented fibrils under the elongational flow; the higher the drawdown ratio, the more highly oriented fibrils formed, and the higher the f_s and Δn values of the blend fibers achieved.

The composition dependence of the orientation of PET-2–LCP-2 fibers is presented in Table IV. Compared with PET-1–LCP-1 fibers, PET-2–LCP-2 fibers are different in that both the f_s and Δn values increase with the content of LCP-2. It may reasonably ascribe to their different chemical structure; the LCP-2 has more rigid chain than LCP-1, as a result, the relaxation time for molecular motion of LCP-2 is longer than that for LCP-1.[10] Therefore, the longer the relaxation time, the higher orientation of molecules developed in the capillary entrance to be retained at the exit. Accordingly, there is no WUSS effect occurred in the PET-2–LCP-2 blend fibers.

The orientation of both PET-1–LCP-1 and PET-2–LCP-2 drawn fibers with the composition of 95/5 was listed in Table V. The drawabil-

ity of the blend fibers is good at this composition, and the orientation of the drawn blend fibers is substantially improved with the increase of draw ratio.

X-ray Studies

WAXD patterns of PET-1–LCP-1 and PET-2–LCP-2 fibers are shown in Figures 1 and 2, respectively. There is no equatorial diffractions of the PET component for both as-spun blend fibers, whereas an intense but broad peak centered at a 2θ of about 19.6° for the latter blend fibers (Fig. 2), which is characteristic of the intermolecular packing order of LCP-2 component. In cases of 80PET–20LCP composition, there is a pronounced reflection peak typical of LCP-2 component but no reflection peak for LCP-1. Moreover, there is a gradual increase in the intensity of the LCP-2 reflection with an increase in its content. In cases of the drawn fibers, there are 3 well-defined peaks typical for PET component corresponding to 010, $1\bar{1}0$, and 100 crystal planes. The crystallinity of PET component increases with the draw ratio. Comparing the drawn blend fibers with the control PET fiber, the crystallographic size of PET component in the former is smaller than that of the latter, indicating that the perfectness of the PET crystallites in the blends is lower than that of control PET. In addition, the crystalline structure is also closely related to drawdown ratio of corresponding as-spun fibers.

Morphological Studies

In order to get better insight into the phase morphology developed in the melt spinning process, the scanning electron microscopy (SEM) observation of the cross section for composite fibers was compared in Figures 3–6. It is obvious that PET is immiscible with LCP, and there are 2 distinct phases in the blends. As is shown in Figure 3, LCP-1 exhibits a globule-like or fibrous dispersed phase in the PET matrix, depending on the composition. With an increase in the LCP-1 content, the suspended phases of LCP-1 are agglomerated into larger particles with more regular spherical shape. At 80PET-1–20LCP-1 composition, the LCP-1 component shows a spherical shape with the average size about 5 μm and only little change in the shape with increasing the drawdown ratio.

However, the LCP-2 dispersed phases in the PET-2–LCP-2 blend could easily be deformed into fibrils by applied stress, as shown in Figure 4. The shape and size of the dispersed phase of LCP-2 experience great changes in the spinning process. It can be clearly seen that LCP-2 component in the blend strand shows a spherical shape with a broad dimension distribution but it is deformed into fibrils with a large aspect ratio and a narrow size distribution, as shown for the as-spun blend fibers. Moreover, the dimension of LCP-2 dispersed phase could be further reduced through increasing the drawdown ratio (Fig. 5). Similar results have been observed by other researchers.[11,12] Figure 6 reveals the effect of composition on the PET-2–

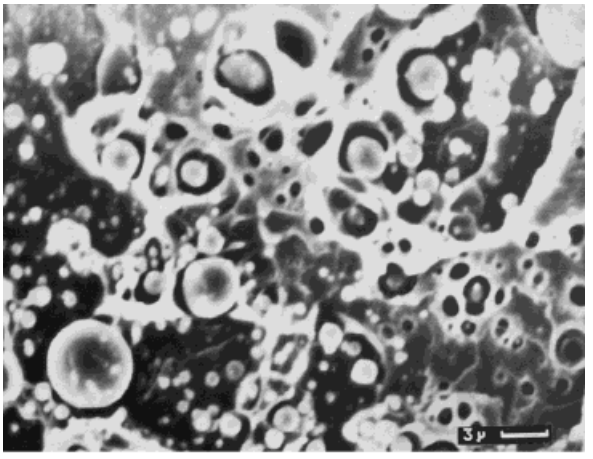

(A)

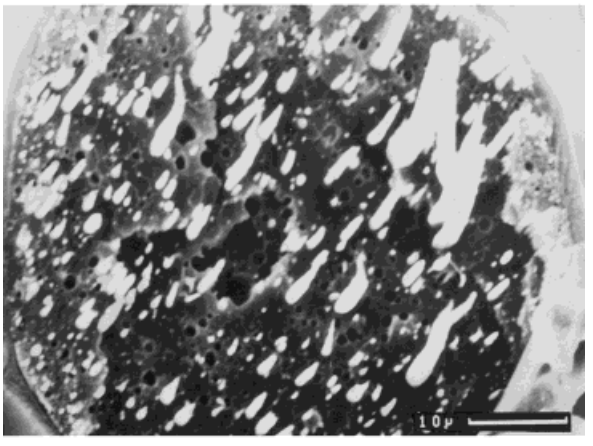

(B)

Figure 4 SEM photographs for 80PET-2–20LCP-2 blend strand and as-spun fiber. (A) Blend strand. (B) As-spun fiber ($V_L/V_0 = 107$).

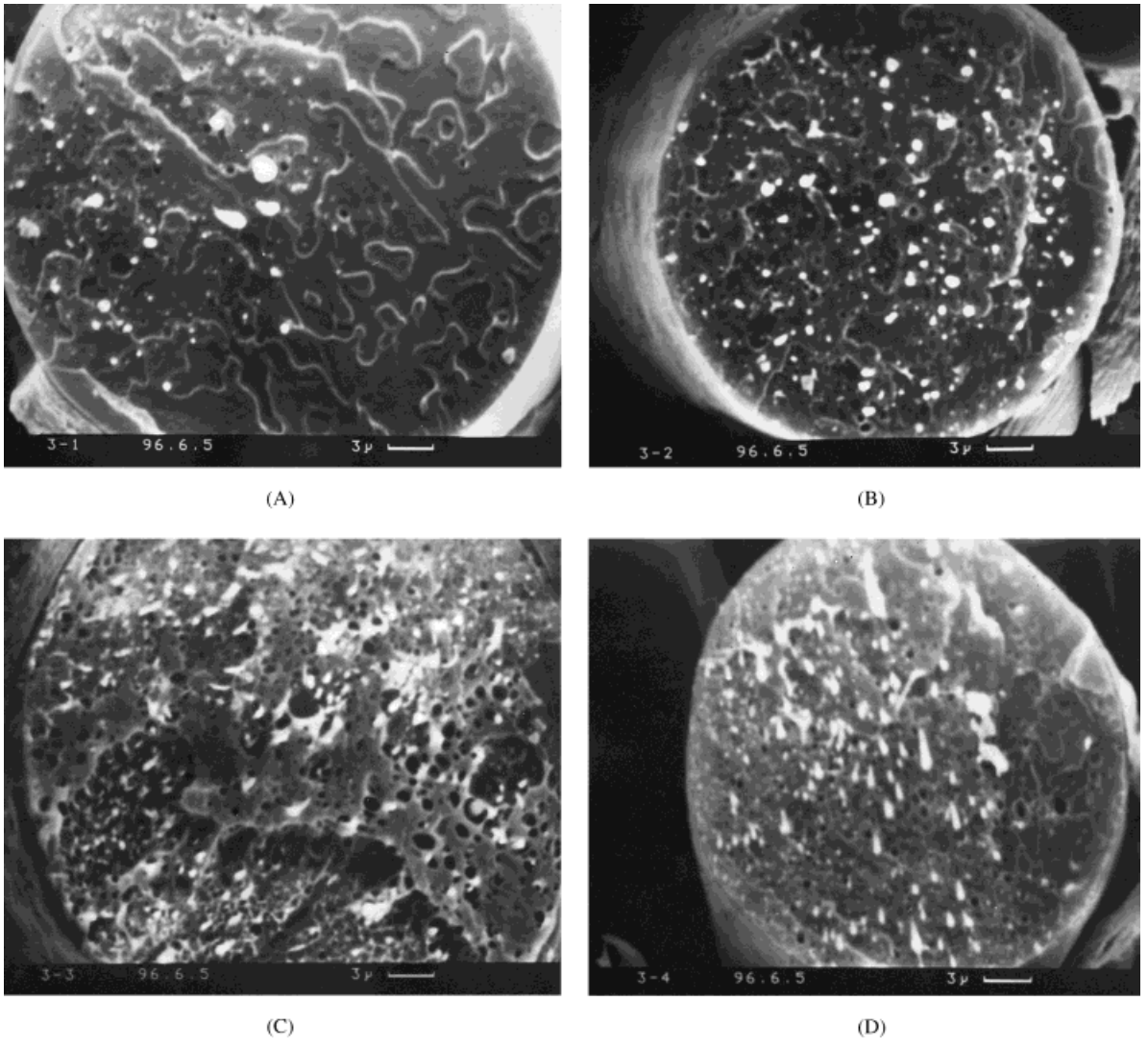

Figure 5 SEM photographs for PET-2–LCP-2 as-spun fibers at various drawdown ratios. (A) 95PET-2–5LCP-2 (V_L/V_0 = 107). (B) 95PET-2–5LCP-2 (V_L/V_0 = 161). (C) 90PET-2–10LCP-2 (V_L/V_0 = 107). (D) 90PET-10LCP–2 (V_L/V_0 = 161).

LCP-2 fiber morphology, which is different from LCP-1 phase morphology in PET-1 matrix: the LCP-2 suspended phase takes a relatively uniform fibrous shape within 20 wt % content of LCP-2. At 50PET-2–50LCP-2 composition, it seems to form a cocontinuous morphology with inclusion of part of a large fibrous LCP-2 in the PET-2 sea or PET-2 in the LCP-2 sea. An obvious phase inversion is observed for the 20PET-2–80LCP-2 composition, which shows a fibrillar morphological feature of LCP-2 matrix because of its easy orientation.

The molecular weight (or intrinsic viscosity) of PET matrix is also an important factor for controlling the blend morphology, as shown in Figure 7. It can be viewed that the LCP-2 exists as a rod-like dispersed phase in PET-1 matrix similar to that in PET-2, however, the dimension of which is much larger in the former case than in the latter one. It is considered that the viscosity ratio of LCP-2 to PET-1 is higher than that of LCP-2 to PET-2, which has a higher intrinsic viscosity; in general, the lower the viscosity ratio, the easier the dispersed phases to be deformed into fine fibrils. By comparison of Figure 3 with 7 for the 90PET–10LCP composition, we could clearly see that LCP-1 component appears as droplets with an average dimension

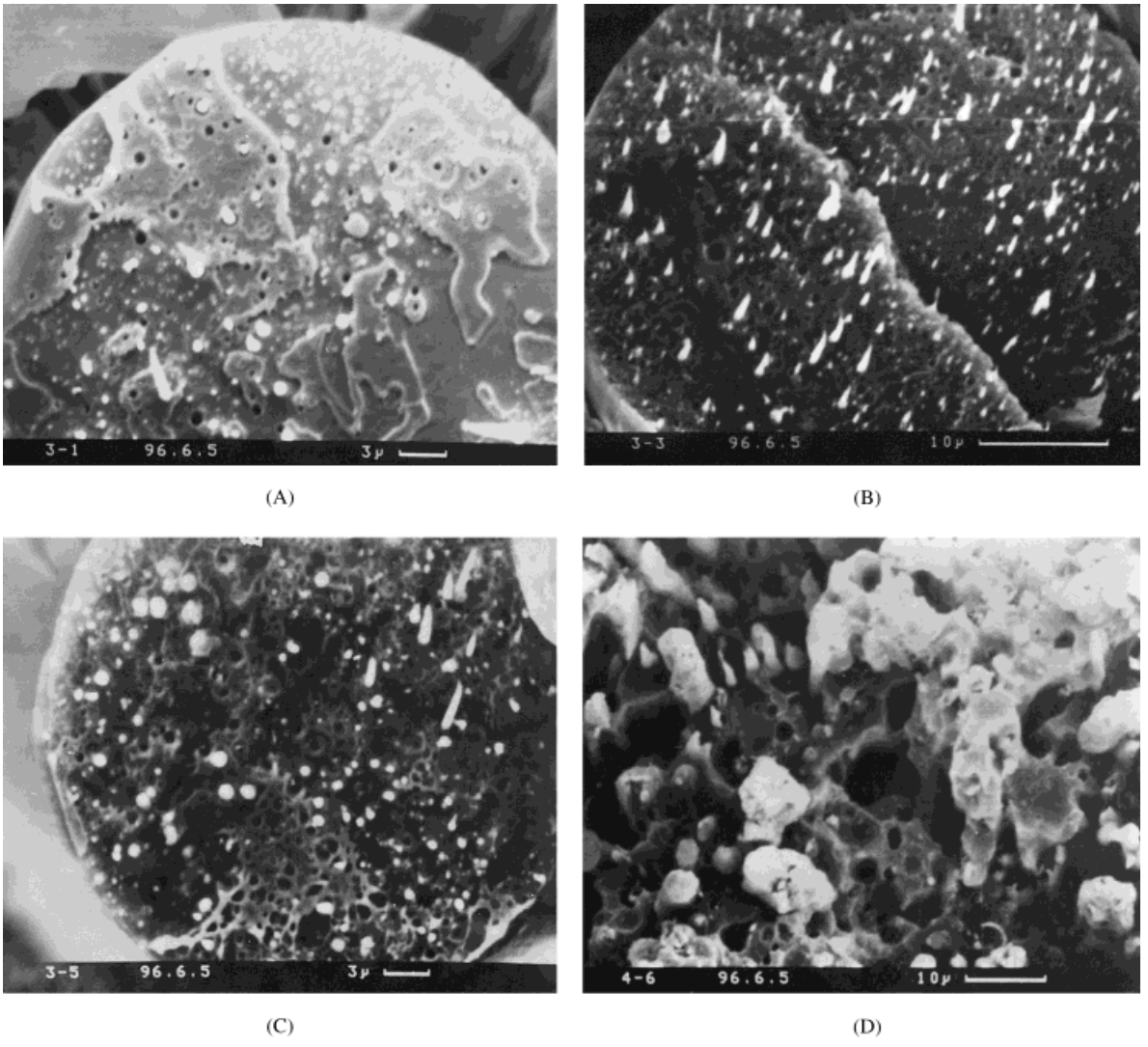

Figure 6 SEM photographs for PET-2–LCP-2 as-spun fibers at the cross section. (A) 95PET-2–5LCP-2. (B) 90PET-2–10LCP-2. (C) 80PET-2–20LCP-2. (D) 50PET-2–50LCP-2. (E) 20PET-2–80LCP-2. (F) 10PET-2–90LCP-2.

about 3.0 μm, whereas LCP-2 exists as fibrous rods with about 2.0 μm size; furthermore, the difference becomes larger with the increase of LCP content in the blends. It could be reasonably ascribed to the difference in the chain rigidity since it will result in different rheological behaviors, as reported in the literature.[2,13]

Mechanical Properties of Blend Fibers

From the morphological analysis above, we find that with the LCP-2 dispersed phase, it is much easier to produce discontinuous fibrils with relatively large aspect ratio in PET matrix than with LCP-1. According to the composite theory, when the higher modulus component forms a continuous phase, a linear rule of mixture for a composite system in the linear elastic range will be the appropriate model, as follows:

$$E_c = E_1V_1 + E_2V_2 \quad (1)$$

where E_c, E_1, and E_2 are the moduli of the composite, PET, and LCP, respectively, and V_1 and V_2 are the corresponding volume fractions. In the case of discontinuous fibrillar morphology, a semiempirical Halpin–Tsai model[14–16] could be applied, the relationship of which is as follows:

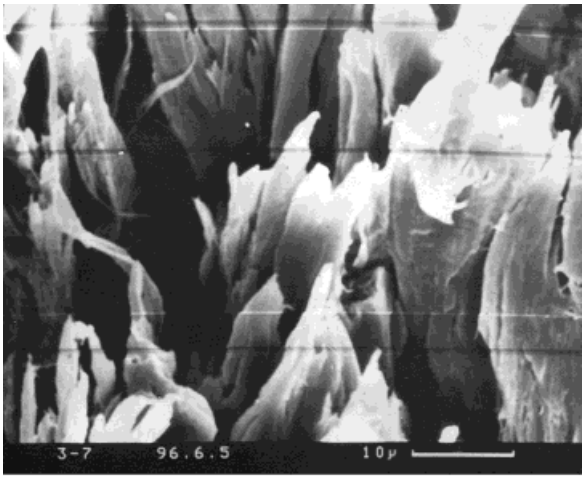

(E)

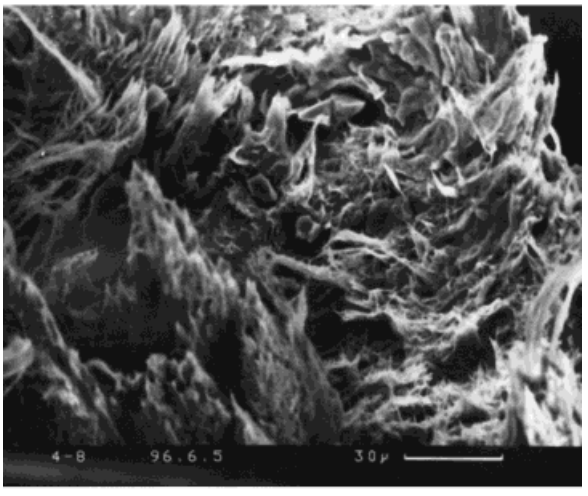

(F)

Figure 6 (*Continued from the previous page*)

$$\frac{E_c}{E_1} = \frac{1 + ABV_2}{1 - B\Psi V_2} \tag{2}$$

where

$$B = \frac{(E_2/E_1) - 1}{(E_2/E_1) + A}, \quad \Psi = 1 + \frac{1 - \Phi_m}{(\Phi_m)^2} V_2$$

where Φ_m is the maximum volume fraction for perfectly aligned discontinuous fibrils, Φ_m is 0.82,[17] and A is equal to twice the average aspect ratio (L/D) of the dispersed phase for completely aligned fibrils.[18]

By measuring the moduli of PET and LCP fibers, respectively, we obtained the modulus values of PET fiber being 1.2 GPa and LCP being 68.0 GPa. The moduli of the blend fibers are then calculated according to their compositions based on equations (1) and (2) and compared with the experimental results (Fig. 8). It is found that for as-spun fibers, the PET-1–LCP-2 approaches the theoretic curve with an average aspect ratio about 10, whereas the PET-2–LCP-2 fits that with the aspect ratio of 29; and for drawn fibers, the actual moduli lie between the upper line predicted by the rule of mixture and the intermediate curve calculated for aspect ratio of 29. The increase of the aspect ratio of the dispersed phase in blend fibers could result in a modulus enhancement.

The molecular weight effect of PET matrix on the strength of as-spun blend fibers is shown in Figure 9. The as-spun fibers with PET-2 as matrix have greatly improved values of strength. The PET-2 blend fiber with 20 wt % LCP has a strength of about 0.20 GPa as compared to 0.08 GPa for control PET-2 fiber. The mechanical improvement may be due to good dispersion of LCP-2 fibrils with a relatively higher aspect ratio,[19] while the PET-1 blend fibers with LCP-2 have much lower strength values due to the lower aspect ratio of the fibrils formed, as mentioned above. The drawing effect is pronounced in strength enhancement, and the improvement is closely related to the blend compositions.

CONCLUSIONS

A different chain structure of LCP has a significant effect on the structure and properties of PET–LCP *in-situ* composite fibers. The addition of LCP-1 with a less rigid chain results in lowering the orientation of as-spun composite fibers, while fibers containing LCP-2 with rod-like rigid chain have a higher orientation than the control PET fiber. Fibers containing LCP-2 have a more pronounced LCP reflection than those containing LCP-1 on the WAXD curves. Drawn composite fibers have less perfect crystals with smaller crystal size than drawn PET control fiber. The chain rigid of LCPs also affects the morphology of PET–LCP composite fiber to a great extent. The morphology of composite fibers with LCP-1 mainly exhibits a spherical phase and a tendency of coagulation with increasing LCP-1 content, while

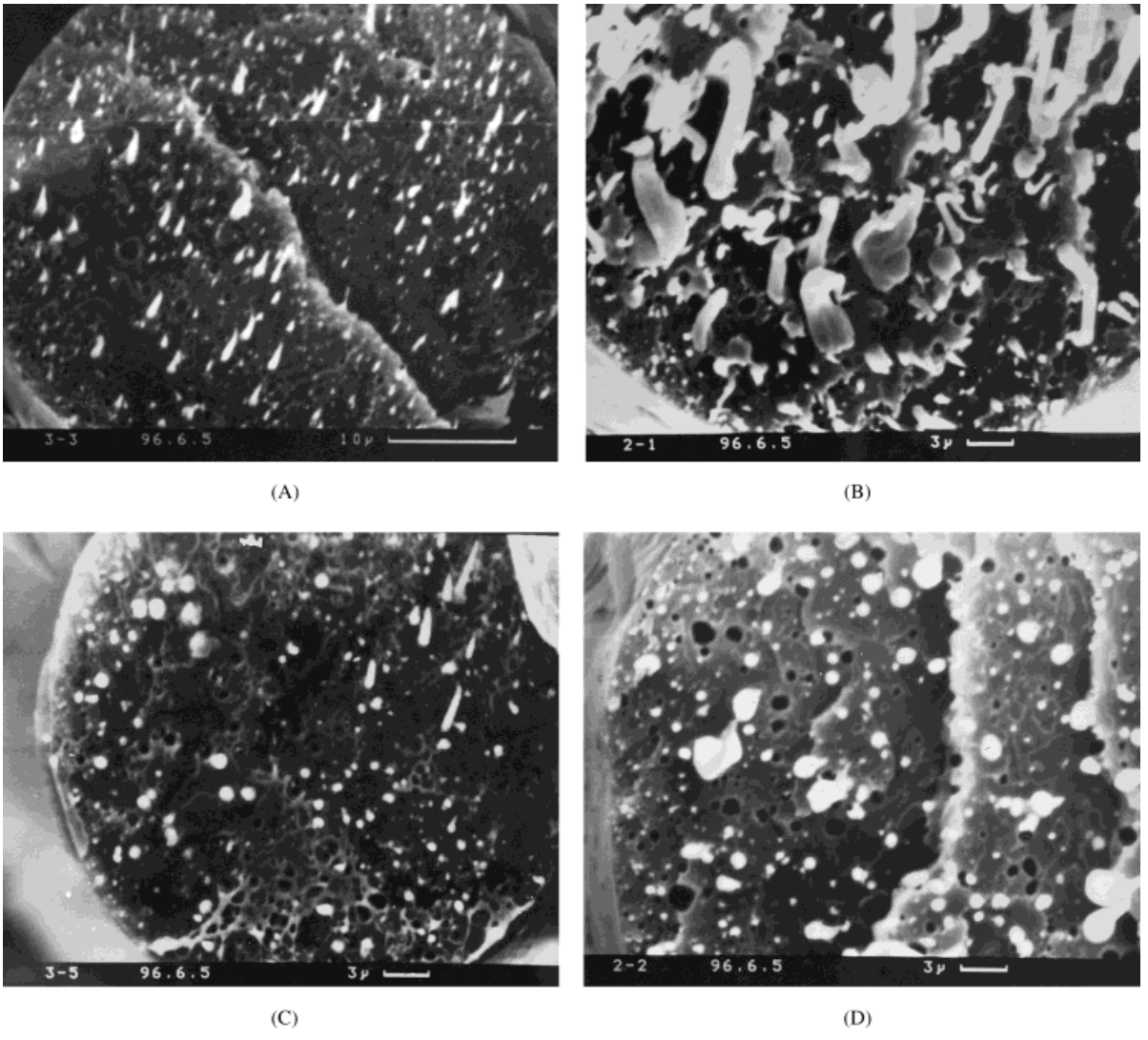

Figure 7 SEM photographs of (A) 90PET-2–10LCP-2; (B) 90PET-1–10LCP-2; (C) 80PET-2–20LCP-2; (D) 80 PET-1–20LCP-2.

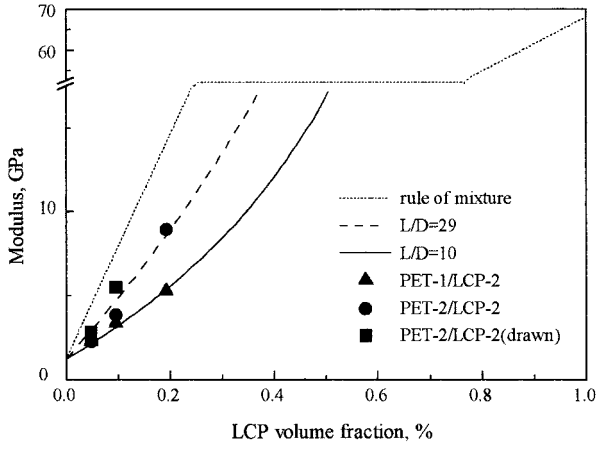

Figure 8 The comparison between the moduli of PET–LCP-2 fibers calculated from the Halpin–Tsai model and that of experimental results.

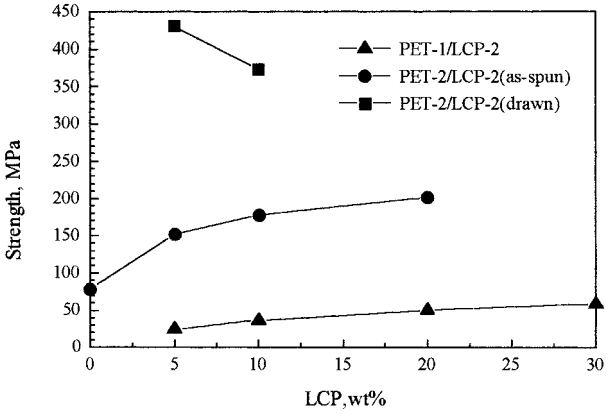

Figure 9 The relationship between the strength and composition of PET–LCP-2 fibers.

LCP-2 shows a fibrillar dispersed phase with a uniform distribution over the composition within 20 wt % LCP-2. Of the most importance, LCP-2 phases could be more readily deformed into fibrils in the PET matrix than LCP-1 during melt processing. This fibril morphology of LCP-2 with a higher aspect ratio leads to an enhancement of mechanical properties of PET–LCP-2 composite fibers. The moduli of PET–LCP-2 blend fibers are described well by the Halpin–Tsai model for short aligned fibers.

The authors thank the National Natural Science Foundation for the support of the research work.

REFERENCES

1. G. Kiss, *Polym. Eng. Sci.,* **27,** 410 (1987).
2. P. Zhuang, T. Kyu, and J. L. White, *Polym. Eng. Sci.,* **28,** 1095 (1988).
3. J. Li, M. Silverstein, A. Hiltner, and E. Baer, *J. Appl. Polym. Sci.,* **44,** 1631 (1992).
4. A. Mithal, A. Tayebi, and C. Lin, *Polym. Eng. Sci.,* **31,** 1533 (1991).
5. S. Mehta and B. L. Deopura, *Polym. Eng. Sci.,* **33,** 931 (1993).
6. S. Joslin, W. Jackson, and R. Farris, *J. Appl. Polym. Sci.,* **54,** 289 (1994).
7. A. M. Sukahadia, D. Done, and D. G. Baird, *Polym. Eng. Sci.,* **30,** 519 (1990).
8. B. Liang and L. Pan, *J. Appl. Polym. Sci.,* **66,** 217 (1997).
9. H. Brody, *J. Appl. Polym. Sci.,* **31,** 2753 (1986).
10. Y. Ide and Z. Ophir, *Polym. Eng. Sci.,* **23,** 261 (1983).
11. K. G. Blizard and D. G. Baird, *Polym. Eng. Sci.,* **27,** 653 (1987).
12. A. Kohli, N. Chung, and R. A. Weiss, *Polym. Eng. Sci.,* **29,** 573 (1989).
13. M. T. Heino, P. T. Hietaoja, T. P. Vainio, and J. V. Seppala, *J. Appl. Polym. Sci.,* **51,** 259 (1994).
14. R. M. Jones, *Mechanics of Composite Materials,* McGraw-Hill, New York, 1975.
15. L. E. Nielsen, *Mechanical Properties of Polymers and Composites,* Marcel Dekker, New York, 1975.
16. H. S. Park and T. Kyu, *Polym. Compos.,* **10,** 421 (1989).
17. L. E. Nielsen, *Mechanical Properties of Polymers and Composites,* Vol. 2, Marcel Dekker, New York, 1981, Chap. 7.
18. L. E. Nielsen, *Mechanical Properties of Polymers and Composites,* Vol. 2, Marcel Dekker, New York, 1981, Chap. 8.
19. B. Y. Shin and I. J. Chung, *Polym. Eng. Sci.,* **30,** 1613 (1990).